



Stiffness, Ultimate Strength Capacity and Cyclic Loading Deterioration Characteristics of Two Different Wood-Structure Dwellings Following The Current Japanese Practice

T. Takahashi⁽¹⁾, T. Nagae⁽²⁾, S. Uwadan⁽³⁾, C. Yenidogan⁽⁴⁾⁽⁵⁾, S. Yamada⁽⁶⁾,
H. Kashiwa⁽⁷⁾, K. Hayashi⁽⁸⁾, T. Inoue⁽⁹⁾

⁽¹⁾ Senior Researcher, NIED, takehiro@bosai.go.jp

⁽²⁾ Associate Professor, Nagoya University, nagae@nagoya-u.jp

⁽³⁾ Graduate Student, Nagoya University

⁽⁴⁾ JSPS Fellow, Nagoya University, cem.yenidogan@gmail.com

⁽⁵⁾ Assistant Professor, Bahçeşehir University, cem.yenidogan@eng.bau.edu.tr

⁽⁶⁾ Associate, NIKKEN SEKKEI LTD, shohei.yamada@nikken.jp

⁽⁷⁾ Senior Researcher, NILIM, kashiwa-h92ta@mlit.go.jp

⁽⁸⁾ Assistant Professor, Toyohashi University of Technology, hayashi@ace.tut.ac.jp

⁽⁹⁾ Deputy Director, NIED, dinoue@bosai.go.jp

Abstract

Two Grade-3 index buildings were designed and constructed according to the current Japanese seismic design guidelines. One was a Post-and-Beam Structure (A-building), and another a Shear-Wall structure (B-building). The sills, column bases and wall bases were anchored to reinforced concrete foundations by steel anchor bolts, thereby fulfilling the guideline requirements. The foundations were firmly fixed, and shaking table motions were fully applied to the foundations. JMA-Kobe motion and JR-Takatori motion recorded in the 1995 Kobe earthquake were used for the ultimate state tests. The two test buildings had stiffness more than two times higher than the design evaluations. The ultimate strength capacities were more than four times that of the allowable stress design capacity.

Keywords: Shaking table test, Wood house, Soil-structure interaction, Functionality, Base isolation

1. Introduction

Comprehensive seismic performance assessment of wood dwellings located in densely populated urban areas was selected as a target of the current E-Defense tests regarding the Tokyo Metropolitan Resilience Project (2017-2022). “The 2019 full-scale shake table test program of wood dwellings” is summarized with the entire test results.^[1] This paper focuses on the evaluations of stiffness, ultimate strength capacity and cyclic loading deterioration characteristics of two different wood buildings shown in Fig. 1.



(1) Construction site (outside west yard)



(2) Completion of setups in E-Defense

Fig. 1 Construction and setup of two wood test buildings (January, 2019)



Two test buildings were designed according to the current Japanese design guidelines. One was a Post-and-Beam Structure (A-building), and another a Shear-Wall structure (B-building). The upper structures were placed on stiff reinforced concrete foundations. The foundations were designed by assuming general soil properties. The sills, column bases and wall bases were anchored by steel anchor bolts, thereby fulfilling the current guideline requirements. The foundation slabs were firmly fixed so that shaking table motions were fully applied to the foundation slabs.

2. Test Building

Figure 2 shows the plans of the first, second and third floors adopted for both A-building and B-building. The two test buildings had identical configurations and plans. Regarding the Post-and-Beam Structure (A-building), braces were fixed by metal connection reinforcement. Structural plywood was fixed by nails. The exterior wall was finished by siding boards. Gypsum board was fixed by screws to the interior side. The exterior wall was finished by wall cloth. The Shear-Wall structure (B-building) adopted prefabricated wall panels composed of a vertical frame, lateral frame and plywood. The siding board, gypsum board and wall cloth were the same in both test buildings. Figure 3 shows the construction process of the test buildings.

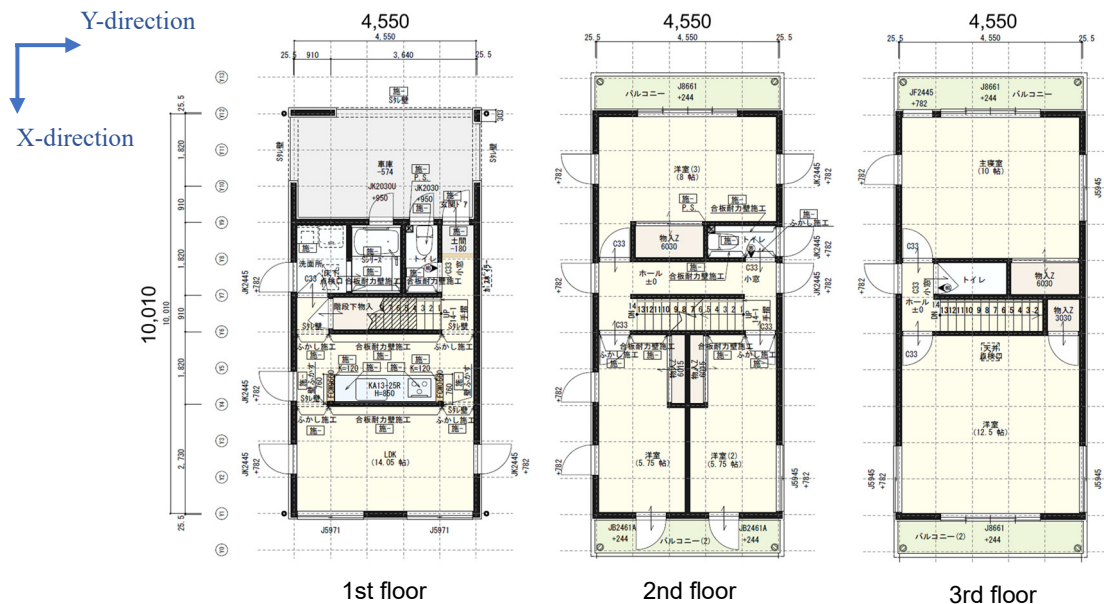


Fig. 2 Plans of A-building and B-building



(1) Post-and-Beam Structure / A-building



(2) Shear-Wall Structure / B-building



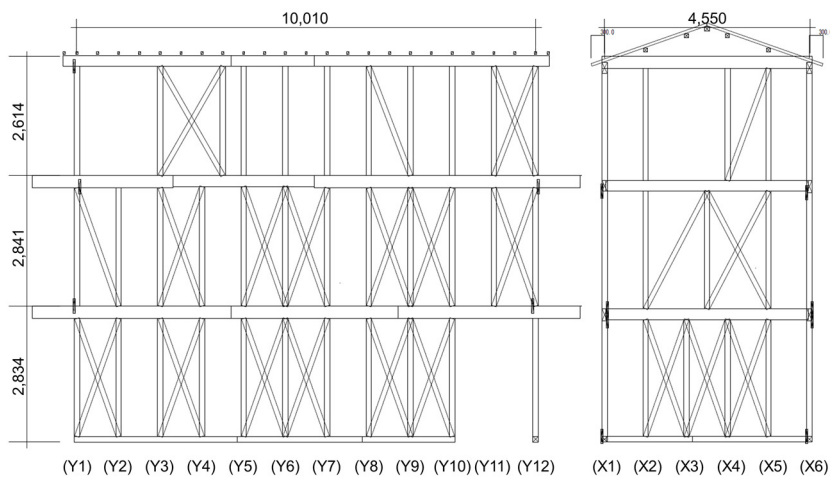
Fig. 3 Construction process of two test buildings (Photos: November-December, 2018)



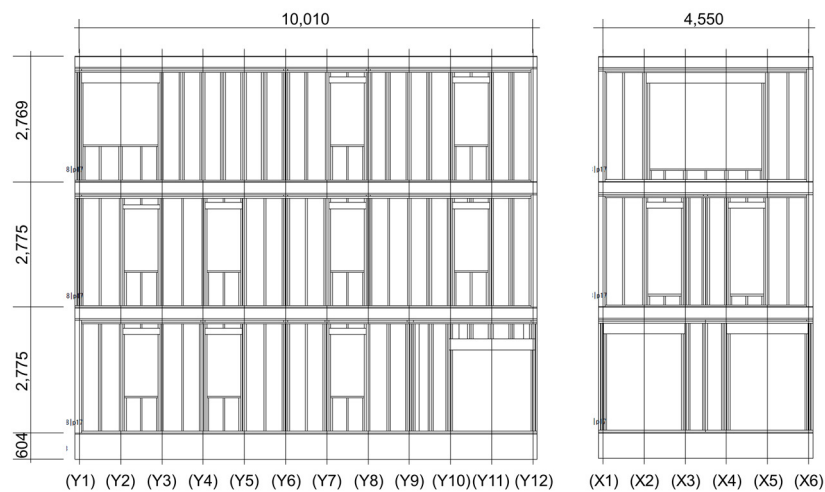
Table 1 shows the seismic force used in the designs of A-building and B-building. Figure 4 shows the framing elevation. For both buildings, the design of the Grade-3 index building was adopted so that the strength

Table 1 Seismic force in the design

A-building	Total weight Σwi (kN)	A_i	Shear force coefficient C_i	Seismic force eQi (kN)
3rd story	79.57	1.603	0.481	38.25
2nd story	230.88	1.207	0.362	83.63
1st story	382.22	1.000	0.300	114.67
B-building	Total weight Σwi (kN)	A_i	Shear force coefficient C_i	Seismic force eQi (kN)
3rd story	79.91	1.60	0.480	38.32
2nd story	226.83	1.21	0.363	82.31
1st story	376.50	1.00	0.300	112.95



(1) A-building (Post-and-Beam Structure)



(2) B-building (Shear-Wall Structure)

Fig. 4 Framing elevation

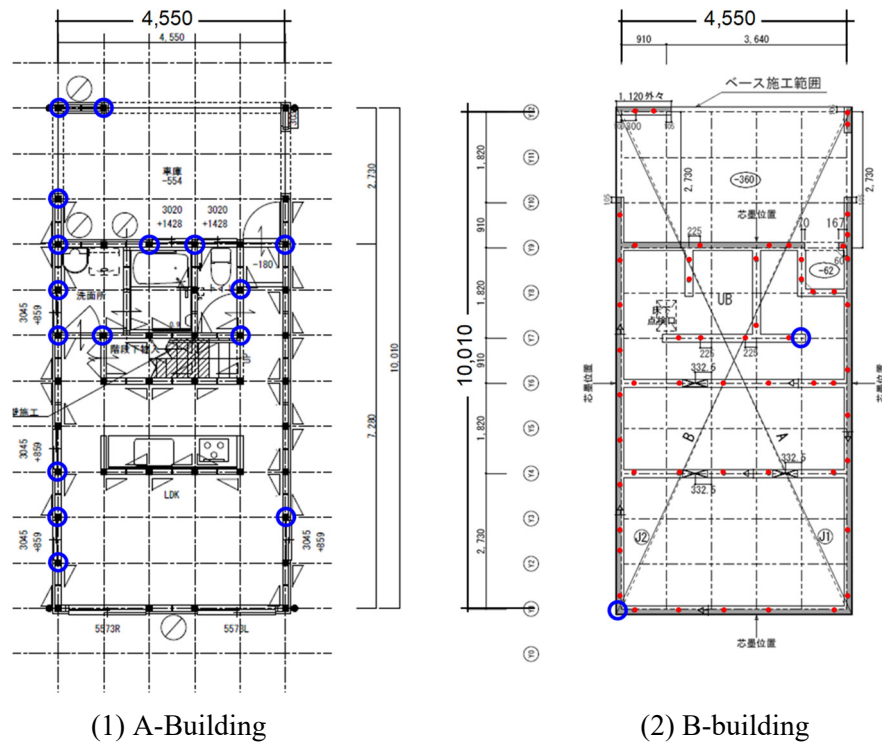


Fig. 5 Locations of steel anchor bolts holding column base

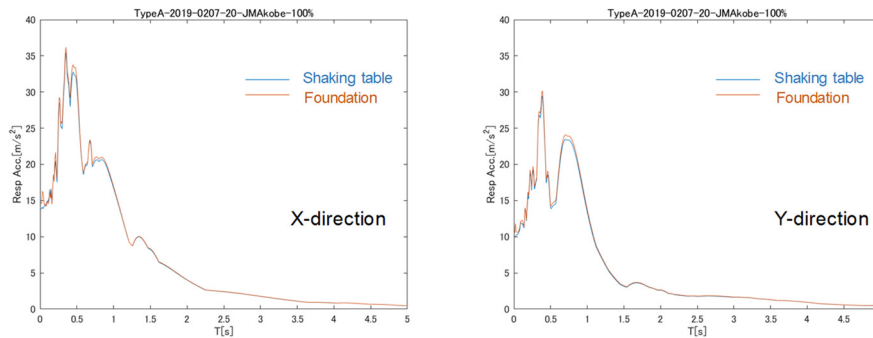
margin to the requirements was minimized. That is, the design stress level to the base shear force coefficient of 0.3 became close to the allowable stress level. Through past experiences of failure modes due to lack of connection strength and column base strength, strict requirements concerning the metal reinforcement for connections and steel anchor bolts holding the column base have been established. Figure 5 shows the locations of steel anchor bolts holding the column base in blue. The equivalent allowable stress design procedures were applied to both the Post-and-Beam Structure (A-building) and Shear-Wall structure (B-building). As a result, the number of steel anchor bolts holding the column base became very different. This is because the tension force in the column base was governed by different design models for the Post-and-Beam and Shear-Wall Structures. The modeling of shear wall panels produced much smaller tension forces in the column bases. Figure 5 (2) shows the locations of anchor bolts fixing the lateral sills to the foundation in red. A-building had the same number of anchor bolts fixing sills to the foundation slab although they are not shown in Fig. 5 (1). The shear wall panels were fixed to sills by nails and metal reinforcements in B-building.

3. Test Results of A-building

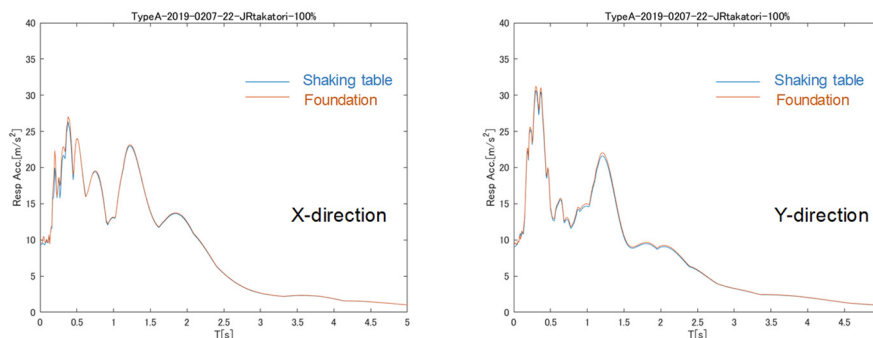
The test program was divided into three phases (Phase 1, Phase 2 and Phase 3), while keeping the same upper structures of the Post-and-Beam Structure (A-building) and Shear-Wall structure (B-building).^[1] A-building was equipped with a base isolation structure in Phase 1. In such condition, the upper structure of A-building had small drift angles of less than 0.003 rad. B-building was supported by a foundation on soil in Phase 1 and Phase 2.^[2] Under such condition, the upper structure of B-building had modest drift angles of less than 0.018 rad. Regarding A-building, the foundation was firmly fixed in Phase 2, while in B-building, it was firmly fixed in Phase 3. JMA-Kobe motion and JR-Takatori motion were used for the tests. In Phase 2, JMA-Kobe 25%, JMA-Kobe 50%, JMA-Kobe 100% and JR-Takatori 100% were used. In Phase 3, JMA-Kobe 100% only was used. The following planned tests were canceled because the ultimate failure occurred in B-building in the first test. This paper focuses on the tests of A-building in Phase 2 and the test of B-building in Phase 3.



Figure 6 shows the acceleration response spectra of the records at the shaking table and foundation for A-building (Phase 2). The orange lines of the foundation are very close to the blue lines of the shaking table. The input motions to the shaking table were fully applied to the foundation.



(1) JMA-Kobe 100%



(2) JR-Takatori 100%

Fig. 6 Acceleration response spectra evaluated at shaking table and foundation slab (A-building of Phase 2)

The maximum inter-story drift angle was limited to less than 0.008 rad in JMA-Kobe 50%. JMA-Kobe 50% is equivalent to the Design-Based Earthquake. On the other hand, when subjected to JMA-Kobe 100%, the response deformation was concentrated on the first story, and the drift angle exceeded 0.03 rad in the X-direction. The maximum inter-story drift exceeded 0.04 rad in the following JR-Takatori 100%. Figure 7 shows the typical damage to the first story after being subjected to JMA-Kobe 100%. In the X-direction, the siding boards fractured in the exterior walls. Significant cracks started at the corners of windows in the interior gypsum boards. In the JR-Takatori 100%, the siding boards spalled from the exterior walls, as shown in Fig.



Fig. 7 Damage to the first story of A-building in the story drift of 0.03 rad (JMA-Kobe 100%)



8 (1). Cracks progressed slightly in the interior walls under cyclic deformations, as shown in Fig. 8 (2). Note that the steel anchor bolts holding the column bases showed maximum strain slightly exceeding 0.2%, and column bases constraint vertical deformations due to tension forces. The first-story deformation comprised mostly of story shear deformation.



(1) Fractured and spalled siding boards came off in the cyclic drift angle of 0.04 rad



(2) Cracks slightly progressed in the interior walls under cyclic deformations

Fig. 8 Video capture of interior and exterior walls when subjected to JR-Takatori 100% (A-building)

Figure 9 shows the relationships between story shear force and story drift angle in each story when subjected to JMA-Kobe 100%. Regarding the first-story relationship, significant inelastic behaviors are shown from the drift angle of 0.01 rad in the X-direction. The maximum strength reached 600 kN at the drift angle of 0.03 rad. Peak orienting shape and pinching shape are observed in the hysteretic loops. In the Y-direction, the maximum drift angle slightly exceeded 0.01 rad, and maximum shear force reached 400 kN. The maximum drift angles were limited to less than 0.01 rad in the second story and less than 0.005 rad in the third story. The maximum shear forces were less than 100 kN in both the X and Y-directions in the third story. Figure 10 shows the relationships when subjected to JR-Takatori 100%. Pinching hysteretic loops are repeatedly depicted. In

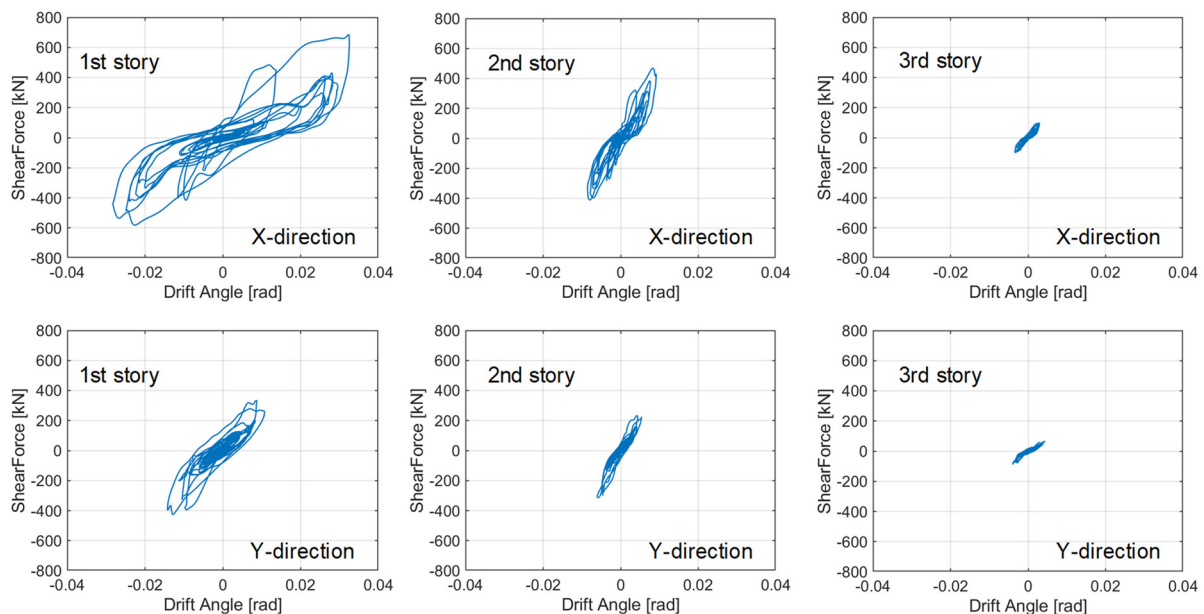


Fig. 9 Relationship between shear force and drift angle in each story of A-building / JMA-Kobe 100%

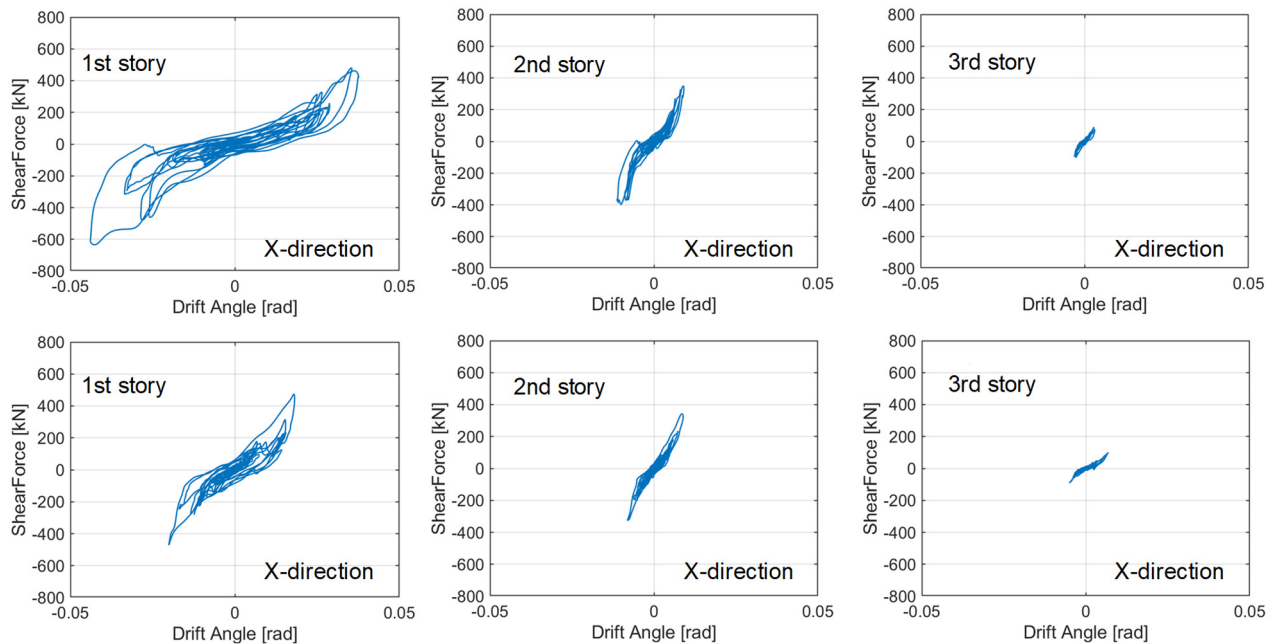


Fig. 10 Relationship between shear force and drift angle in each story of A-building / JR-Takatori 100%

the first story, the maximum shear force exceeded the values experienced in JMA-Kobe 100% on the negative side in the X-direction and on both the positive and negative sides in the Y-direction.

3. Test Results of B-building

When subjected to JMA-Kobe 100%, the table input motion was fully applied to the foundation of B-building. Figure 11 shows the ultimate failure states of B-building. Severe fractures of the wall base occurred at the interface between shear wall panels and sills. Regarding the steel anchor bolts holding the column base, the screws were completely pulled out from the column base. The overviews captured at the moment of the wall base fractures (Fig. 12) indicated that the overturning moment due to significant inertia force in the Y-direction uplifted the south exterior frame. The recorded maximum value of uplifting was more than 400 mm.



Fig. 11 Wall base fracture at the south exterior wall and screws pulled out at column base (B-building after subjected to JMA-Kobe 100%)

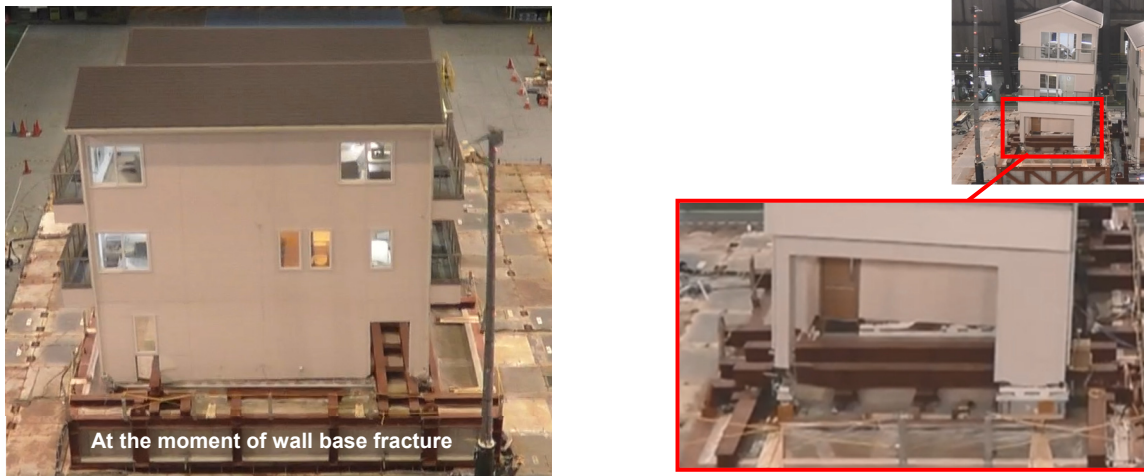


Fig. 12 Overviews of B-building subjected to JMA-Kobe 100%

Figure 13 shows the relationship between the story shear force and drift angle of each story when B-building was subjected to JMA-Kobe 100%. The maximum drift angle reached 0.08 rad in the X-direction, and exceeded 0.1 rad in the Y-direction. Such value was more than two times that of A-building in the X-direction, and more than three times that of A-building in the Y-direction. The response deformations were significantly concentrated on the first story. In the large deformation ranges, steep negative slopes are depicted, and the shear force decreased to less than 20% of the maximum shear force in each of the X and Y-directions.

Figure 14 shows the relationship between the overturning moment and rocking rotation angle at the wall base level when subjected to JMA-Kobe 100%. The horizontal dotted line shows the resisting moment due to the total weight of the upper structure. This is evaluated as the product of the total weight (376.50 kN) and the half-length of the structural plane (X-direction: 10,010/2 mm, Y-direction: 4,550/2 mm). After the overturning moment significantly exceeded the weight resisting moment, the hysteretic loop showed a steep negative slope from the peak point. The rotation angle due to rocking exceeded 0.04 rad in the Y-direction. The overturning moment decreased to less than 20% from the peak due to the brittle wall base fracture.

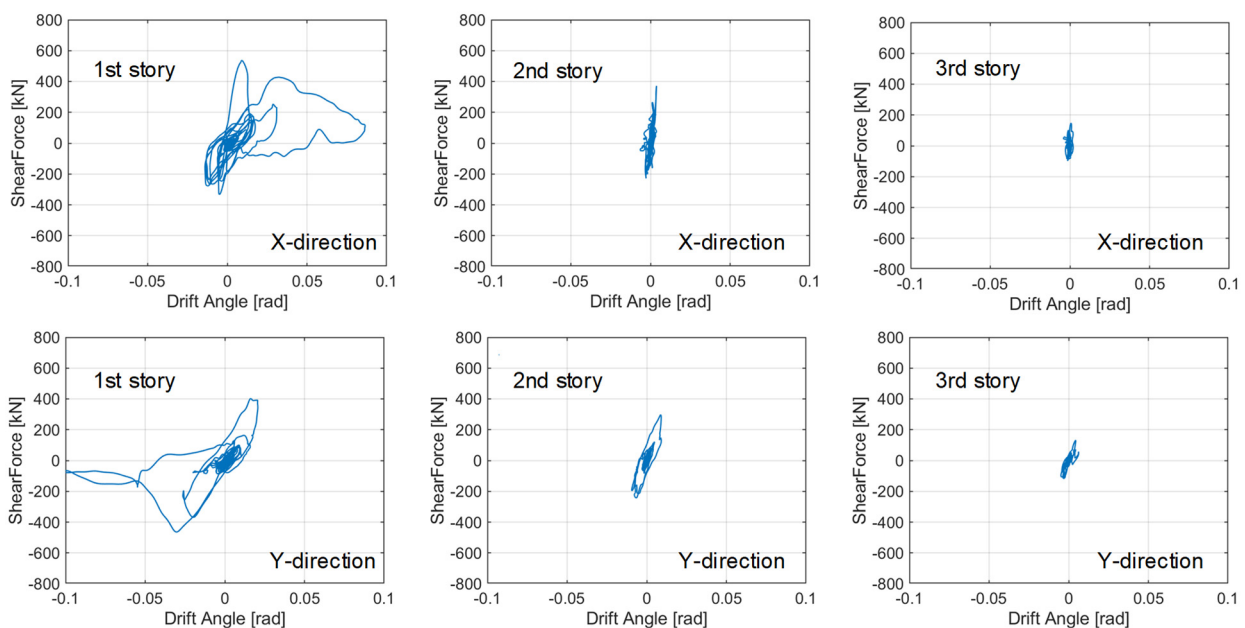


Fig. 13 Relationship between story shear force and drift angle (B-building in JMA-Kobe 100%)

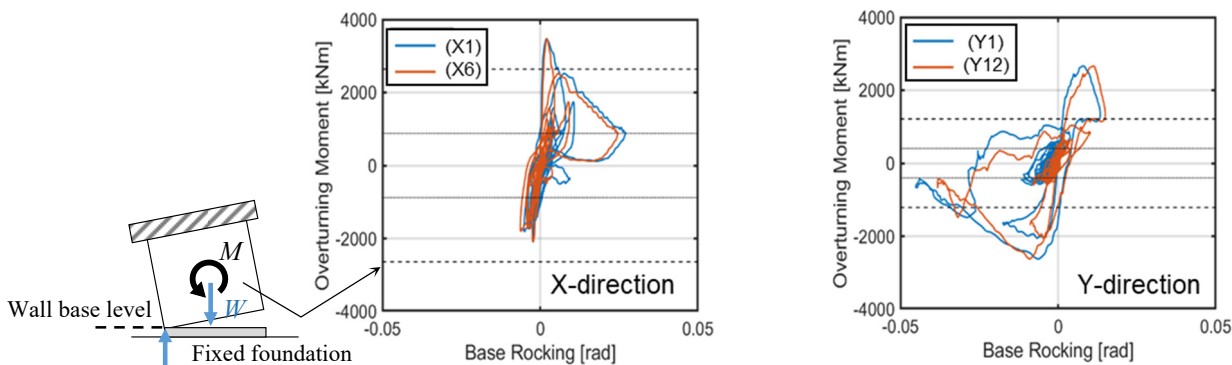
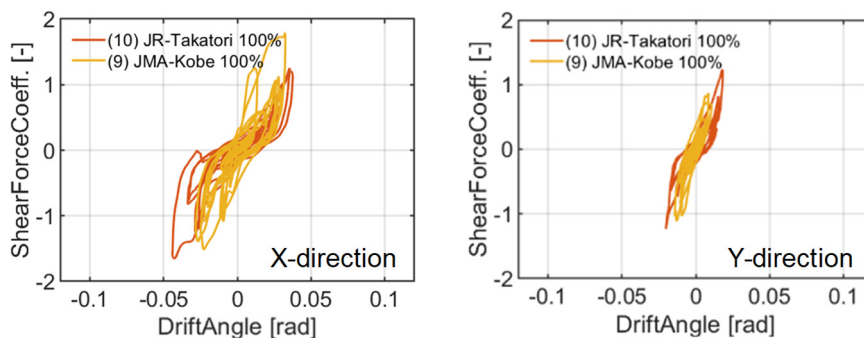


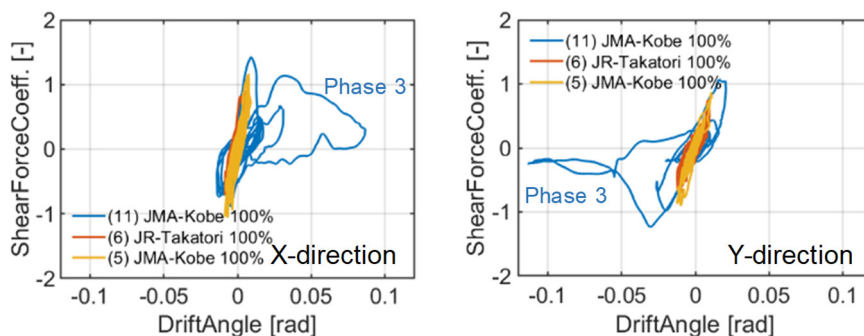
Fig. 14 Relationship between overturning moment and rocking rotation angle at wall base level (B-building subjected to JMA-Kobe 100%)

5. Stiffness and Strength Capacity

Figure 15 shows the relationship between the base shear force coefficient and drift angle. The results of sequential tests are shown together in the same graph. Regarding A-building shown in the upper part of Fig. 15, the maximum strength capacity is correspondent to the base shear force coefficient of 1.8 in the X-direction and 1.2 in the Y-direction. Regarding B-building shown in the lower part of Fig. 15, the maximum strength capacity is correspondent to the base shear force coefficient of 1.4 in the X-direction and 1.2 in the Y-direction. In design practice, the story stiffness is checked at the drift angle of 1/150 rad. Compared to such design values, the test results reached values about two times higher. The allowable stress design for the Grade 3 index building adopts the base shear coefficient of 0.3 as the seismic design force. Compared to such allowable stress



(1) A-building



(2) B-building

Fig. 15 Relationship between the base shear force coefficient and drift angle



capacities required in design, the ultimate strength capacities reached a value four times higher. Especially in the X-direction of A-building, the strength capacity had the largest margin by a value six times higher.

6. Conclusions

Two Grade-3 index buildings were designed and constructed base on the current Japanese seismic design guidelines in order to assess their ultimate states, stiffness and deteriorating behaviors. Two three-story test buildings represented typical Japanese current constructions seen in densely populated urban areas. One adopted the Post-and-Beam Structure, and the other the Shear-Wall structure. The sills, column bases and wall bases were anchored to the reinforced concrete foundations by steel anchor bolts, thereby fulfilling the guideline requirements. The foundations were firmly fixed, and shaking table motions were fully applied to the foundations. JMA-Kobe motion and JR-Takatori motion recorded in the 1995 Kobe earthquake were used for the sequential tests. The test buildings represented stiffness more than two times higher than the design evaluations. Regarding A-building, the maximum inter story drift angle was limited to less than 0.008 rad in JMA-Kobe 50%, which is equivalent to the Design-Based Earthquake. However, when subjected to JMA-Kobe 100%, the response deformations were concentrated on the first story, and exceeded the drift angle of 0.03 rad. The story deformation was mainly comprised of story shear deformation. In the deformation range exceeding 0.01 rad, the hysteretic loops depicted peak orienting shape and pinching shape. The ultimate strength capacities were more than four times the allowable stress design capacity of the Grade-3 index building. Regarding B-building, severe fractures of wall bases occurred at the interface between the sill and wall panel. During the test of JMA-Kobe 100%, the overturning moment of the upper structure exceeded the weight resisting moment capacity at the wall base. Thus, the wall base was short of steel anchor bolts holding the column base. The tension forces to the wall and column base are governed by the component models. The Shear-Wall Structure produced much smaller tension forces in the allowable stress design. The maximum strength capacities reached four times the allowable stress design capacity of the Grade-3 index building. After exceeding the ultimate fracture state, significant strength deterioration occurred, and the steep negative slope ended at a point of less than 20% of the maximum strength capacity.

7. Acknowledgements

This work is supported by the Tokyo Metropolitan Resilience Project of the National Research Institute for Earth Science and Disaster Resilience (NIED). Collaboration on earthquake engineering research using E-Defense and NHERI facilities is proceeding continuously. Construction of the test buildings was managed by ICHIJO Co., Ltd. Test-relevant affairs were administrated by the Graduate School of Environmental Studies, Nagoya University and E-Defense, NIED.

8. References

- [1] T. Nagae, S. Uwadan, C. Yenigodan, S. Yamada, H. Kashiwa, K. Hayashi, T. Takahashi, T. Inoue (2020): The 2019 full-scale shake table test program of wood dwellings. *17th World Conference on Earthquake Engineering, 17WCEE*, Paper No. C002274.
- [2] T. Nagae, S. Uwadan, K. Takaya, C. Yenidogan, S. Yamada, H. Kashiwa, K. Hayashi, T. Takahashi, T. Inoue (2020): Sliding-rocking combined actions at base foundation influencing global and local deformations of upper wood structure. *17th World Conference on Earthquake Engineering, 17WCEE*, Paper No. C002277.